NATIONAL ADVISORY COMMITTEE FOR AERONAUTICS

TECHNICAL NOTE

No. 1486

STRESS DISTRIBUTION IN A BEAM OF ORTHOTROPIC MATERIAL SUBJECTED TO A CONCENTRATED LOAD

By C. B. Smith and A. W. Voss

Forest Products Laboratory

Washington
March 1948

NATIONAL ADVISORY COMMITTEE FOR AERONAUTICS

TECHNICAL NOTE NO. 1486

STRESS DISTRIBUTION IN A BEAM OF ORTHOTROPIC MATERIAL SUBJECTED TO A CONCENTRATED LOAD

By C. B. Smith and A. W. Voss

SUMMARY

Mathematical expressions have been derived for the stress distribution in a wood beam of rectangular cross section subjected to a concentrated load. The orthotropic nature of wood was taken into account in the derivation. The stress distributions were expressed in terms of infinite series. A method of reducing the infinite series to the sum of a finite series and a closed form was described.

The mathematically determined distribution of horizontal shear in the vicinity of a concentrated load was compared with the actual distribution obtained by a test of a Sitka spruce beam of rectangular cross section.

INTRODUCTION

A number of experiments on the bending of wood beams conducted at the Forest Products Laboratory have shown some results that are not explainable by the elementary theory of bending. It is well known that the state of stress that is produced in the interior of a beam, slightly bent by any forces, may be approximated by the elementary theory of bending at all points that are at a considerably large distance from any place of loading or of support. But the stress distribution near a concentrated load or a place of support is not easily determined. Hence, in applying the usual beam theory to wood beams, discrepancies occur in the neighborhood of concentrated loads. This analysis is an attempt to present for wood beams a more nearly exact mathematical derivation of the stress distribution near a concentrated load that is obtained from the elementary theory of bending, in order to explain some of the discrepancies that may arise in the bending of wood beams.

This work was conducted at the Forest Products Laboratory under the sponsorship and with the financial assistance of the National Advisory Committee for Aeronautics.

MATHEMATICAL ANALYSIS

Method of Analysis

The beam discussed is assumed to be an orthotropic solid in the form of a long, thin, rectangular plate having its edges parallel to two perpendicular axes of elastic symmetry lying in the plane of the plate. In the analysis wood is considered to be orthotropic. (See references 1, 2, and 3.) For mathematical simplicity the thickness of the beam is assumed small as compared with the vertical depth of the beam so that the problem can be treated as one of plane stress.

The beam is taken to be infinitely long and to be subjected to a periodic normal load on the upper and lower faces (references 4 and 5). The results obtained are then extended to various types of loading and end conditions for a beam of finite length. The formulas obtained apply to beams of any thickness that is small in comparison with the depth if the load is considered to be given per unit thickness.

The x-axis is taken along the middle line of the beam, and the equation of the upper and lower faces of the beam is taken to be $y = \pm h$, as shown by figure 1.

Sinusoidal Loading of an Infinite Beam

For the state of plane stress in the orthotropic beam, the stress function is given by a suitable solution of the following differential equation. (See reference 6.)

$$\frac{\partial^4 F}{\partial x^4} + 2\kappa \frac{\partial^4 F}{\partial x^2 \partial \eta^2} + \frac{\partial^4 F}{\partial \eta^4} = 0 \tag{1}$$

where

$$\kappa = \frac{\sqrt{E_x E_y}}{2}\left(\frac{1}{\mu_{xy}} - \frac{2\sigma_{xy}}{E_x}\right) \tag{2}$$

and

$$\eta = \epsilon y \tag{3}$$

In equation (3)

$$\epsilon = \sqrt[4]{\frac{E_x}{E_y}} \tag{4}$$

Also,

E_x, E_y moduli of elasticity in x- and y-directions, respectively

μ_{xy} modulus of rigidity associated with xy-plane

σ_{xy} Poisson's ratio associated with stress in x-direction and strains in x- and y-directions

For the components of stress the notation X_x, Y_y, and X_y is used as in reference 7. First the beam is subjected to the surface force

$$\left.\begin{aligned} Y_y &= \tfrac{1}{2}H \cos mx \\ X_y &= 0 \end{aligned}\right\} \tag{5}$$

on the edges $y = \pm h$.

A solution of equation (1) that can be made to satisfy these boundary conditions is

$$F = \left(A_1 \cosh m\alpha\eta + B_1 \cosh m\beta\eta\right) \cos mx \tag{6}$$

where

$$\alpha = \sqrt{\kappa + \sqrt{\kappa^2 - 1}} \qquad \beta = \sqrt{\kappa - \sqrt{\kappa^2 - 1}} \tag{7}$$

and it is important to note that $\alpha\beta = 1$.

The resulting stress components are

$$\frac{\delta^2 F}{\delta x^2} = Y_y = -m^2 \left(A_1 \cosh m\alpha\eta + B_1 \cosh m\beta\eta\right) \cos mx \tag{8}$$

$$\epsilon^2 \frac{\delta^2 F}{\delta \eta^2} = X_x = \epsilon^2 m^2 \left(A_1\alpha^2 \cosh m\alpha\eta + B_1\beta^2 \cosh m\beta\eta\right) \cos mx \tag{9}$$

$$-\epsilon \frac{\delta^2 F}{\delta x\, \delta \eta} = X_y = \epsilon m^2 \left(A_1\alpha \sinh m\alpha\eta + B_1\beta \sinh m\beta\eta\right) \sin mx. \tag{10}$$

From equation (5), the value of X_y on the surface leads to

$$A_1\alpha \sinh m\alpha\epsilon h + B_1\beta \sinh m\beta\epsilon h = 0$$

or

$$B_1 = -\frac{A_1\alpha \sinh m\alpha\epsilon h}{\beta \sinh m\beta\epsilon h} \tag{11}$$

Also from equation (5), the value of Y_y on the surface leads to

$$-m^2\left(A_1 \cosh m\alpha\epsilon h + B_1 \cosh m\beta\epsilon h\right)\cos mx = \tfrac{1}{2}H \cos mx \qquad (12)$$

On solving equations (11) and (12) for A_1 and B_1, it is found that

$$A_1 = \frac{H\beta \sinh m\beta\epsilon h}{2m^2\left(\alpha \sinh m\alpha\epsilon h \cosh m\beta\epsilon h - \beta \sinh m\beta\epsilon h \cosh m\alpha\epsilon h\right)} \qquad (13)$$

and

$$B_1 = \frac{-H\alpha \sinh m\alpha\epsilon h}{2m^2\left(\alpha \sinh m\alpha\epsilon h \cosh m\beta\epsilon h - \beta \sinh m\beta\epsilon h \cosh m\alpha\epsilon h\right)} \qquad (14)$$

The state of stress is now given by

$$Y_y = -\frac{H}{2D_1}\left(\beta \sinh m\beta\epsilon h \cosh m\alpha\eta - \alpha \sinh m\alpha\epsilon h \cosh m\beta\eta\right)\cos mx \qquad (15)$$

$$X_x = \frac{H\epsilon^2}{2D_1}\left(\alpha \sinh m\beta\epsilon h \cosh m\alpha\eta - \beta \sinh m\alpha\epsilon h \cosh m\beta\eta\right)\cos mx \qquad (16)$$

$$X_y = \frac{H\epsilon}{2D_1}\left(\sinh m\beta\epsilon h \sinh m\alpha\eta - \sinh m\alpha\epsilon h \sinh m\beta\eta\right)\sin mx \qquad (17)$$

where

$$D_1 = \alpha \sinh m\alpha\epsilon h \cosh m\beta\epsilon h - \beta \sinh m\beta\epsilon h \cosh m\alpha\epsilon h$$

Next the boundary conditions are taken to be

$$\left.\begin{aligned} Y_y &= \tfrac{1}{2}H \cos mx \qquad (y = h) \\ Y_y &= -\tfrac{1}{2}H \cos mx \qquad (y = -h) \\ X_y &= 0 \qquad (y = \pm h) \end{aligned}\right\} \qquad (18)$$

A solution of equation (1) that can be made to satisfy these conditions is

$$F = \left(A_2 \sinh m\alpha\eta + B_2 \sinh m\beta\eta\right)\cos mx \qquad (19)$$

and the resulting stress components are

$$\frac{\delta^2 F}{\delta x^2} = Y_y = -m^2\left(A_2 \sinh m\alpha\eta + B_2 \sinh m\beta\eta\right)\cos mx \qquad (20)$$

$$\epsilon^2 \frac{\delta^2 F}{\delta \eta^2} = X_x = \epsilon^2 m^2 \left(A_2 \alpha^2 \sinh m\alpha\eta + B_2 \beta^2 \sinh m\beta\eta \right) \cos mx \tag{21}$$

$$-\epsilon \frac{\delta^2 F}{\delta x m} = X_y = \epsilon m^2 \left(A_2 \alpha \cosh m\alpha\eta + B_2 \beta \cosh m\beta\eta \right) \sin mx \tag{22}$$

From equations (18) and (22) it results that

$$A_2 \alpha \cosh m\alpha\epsilon h + B_2 \beta \cosh m\beta\epsilon h = 0$$

or

$$B_2 = - \frac{A_2 \alpha \cosh m\alpha\epsilon h}{\beta \cosh m\beta\epsilon h} \tag{23}$$

Also from equations (18) and (20), it follows that

$$m^2 \left(A_2 \sinh m\alpha\epsilon h + B_2 \sinh m\beta\epsilon h \right) = - \frac{1}{2} H \tag{24}$$

On solving equations (23) and (24) for A_2 and B_2, it is found that

$$A_2 = \frac{- H\beta \cosh m\beta\epsilon h}{2m^2(\beta \sinh m\alpha\epsilon h \cosh m\beta\epsilon h - \alpha \cosh m\alpha\epsilon h \sinh m\beta\epsilon h)} \tag{25}$$

and

$$B_2 = \frac{H\alpha \cosh m\alpha\epsilon h}{2m^2(\beta \sinh m\alpha\epsilon h \cosh m\beta\epsilon h - \alpha \cosh m\alpha\epsilon h \sinh m\beta\epsilon h)} \tag{26}$$

By substituting from equations (25) and (26), the stress components become

$$Y_y = \frac{H}{2D_2} \left(\beta \cosh m\beta\epsilon h \sinh m\alpha\eta - \alpha \cosh m\alpha\epsilon h \sinh m\beta\eta \right) \cos mx \tag{27}$$

$$X_x = - \frac{H\epsilon^2}{2D_2} \left(\alpha \cosh m\beta\epsilon h \sinh m\alpha\eta - \beta \cosh m\alpha\epsilon h \sinh m\beta\eta \right) \cos mx \tag{28}$$

$$X_y = - \frac{H\epsilon}{2D_2} \left(\cosh m\beta\epsilon h \cosh m\alpha\eta - \cosh m\alpha\epsilon h \cosh m\beta\eta \right) \sin mx \tag{29}$$

where

$$D_2 = \beta \sinh m\alpha\epsilon h \cosh m\beta\epsilon h - \alpha \sinh m\beta\epsilon h \cosh m\alpha\epsilon h$$

For isotropic material, it follows from equations (2), (4), and (7) that α, β, and ϵ are equal to unity. For this value of α, β, and ϵ, the

stresses given in equations (15) to (17) and (27) to (29) reduce to the ones that have been found for the isotropic case. (See references 4 and 5.)

The two problems just solved give pericdic sinusoidal load distributions along the upper and lower faces of the beam. It is now evident that by means of Fourier series the beam can be subjected to a very general type of loading.

Concentrated Loading of an Infinite Beam

Consider first the infinitely long beam acted on by equal and similarly directed loads distributed over equal intervals of length a. This distribution of loads may be regarded as a continuous load of the type

$$\psi(x) = \ldots \phi(x - 2a) + \phi(x - a) + \phi(x) + \phi(x + a) + \phi(x + 2a) + \ldots \quad (30)$$

where $\phi(x)$ is a suitably restricted even function of x. It follows that $\psi(x)$ is an even function of period 2a and that $\psi(x + a) = \psi(x - a) = \psi(x)$. These requirements are satisfied by the type of load used in reference 5, in which the definition of $\phi(x)$ was chosen as

$$\phi(x) = \frac{\delta}{\pi} \frac{1}{x^2 + \delta^2} \quad (31)$$

This expression represents a unit load, since the area between the curve and the x-axis is unity. For small values of δ it is suitable for the approximate representation of a load applied over a small area by a curved loading block. The components of stress associated with a point load are obtained as the limit, as δ approaches zero, of the expressions for these components in terms of the parameter δ. These limiting expressions represent the exact solution of the problem of determining the stress distribution associated with a point load. For finite but small values of δ the expressions for the components of stress give the approximate distribution of stress associated with a load distributed over a small area.

The expression for $\psi(x)$ (equation (30)) can be represented by a Fourier series of the form

$$\psi(x) = b_0 + b_2 \cos \frac{2\pi x}{a} + b_4 \cos \frac{4\pi x}{a} + \ldots \quad (32)$$

where

$$\left.\begin{aligned} b_0 &= \frac{1}{a}\int_0^a \psi(x)\, dx \\ b_r &= \frac{2}{a}\int_0^a \psi(x) \cos \frac{r\pi x}{a}\, dx \quad \left(r = 2, 4, 6 \ldots\right) \end{aligned}\right\} \quad (33)$$

Substituting equation (30) in the first of these integrals gives

$$b_0 = \frac{1}{a}\left[\ldots + \int_0^a \phi(x - 2a)\,dx + \int_0^a \phi(x - a)\,dx + \int_0^a \phi(x)\,dx + \int_0^a \phi(x + a)\,dx + \int_0^a \phi(x + 2a)\,dx + \ldots\right] \tag{34}$$

Let

$$\left.\begin{aligned} x - 2a &= x_{-2} \\ x - a &= x_{-1} \\ x &= x_0 \\ x + a &= x_1 \\ &\ldots \end{aligned}\right\} \tag{35}$$

Then

$$b_0 = \frac{1}{a}\left[\ldots + \int_{-2a}^{-a} \phi(x_{-2})\,dx_{-2} + \int_{-a}^{0} \phi(x_{-1})\,dx_{-1} + \int_0^a \phi(x_0)\,dx_0 + \int_a^{2a} \phi(x_1)\,dx_1 + \int_{2a}^{3a} \phi(x_2)\,dx_2 + \ldots\right]$$

or

$$b_0 = \frac{1}{a}\int_{-\infty}^{\infty} \phi(x)\,dx \tag{36}$$

By similarly substituting equation (30) in the second of the integrals of equation (33), it follows that

$$b_r = \frac{2}{a}\left[\ldots + \int_0^a \phi(x - 2a)\cos\frac{r\pi x}{a}\,dx + \int_0^a \phi(x - a)\cos\frac{r\pi x}{a}\,dx + \int_0^a \phi(x)\cos\frac{r\pi x}{a}\,dx + \int_0^a \phi(x + a)\cos\frac{r\pi x}{a}\,dx + \int_0^a \phi(x + 2a)\cos\frac{r\pi x}{a}\,dx + \ldots\right]$$

where $r = 2, 4, 6 \ldots$.

Again make the change of variable indicated in equation (35). It results that

$$b_r = \frac{2}{a}\left[\ldots + \int_{-2a}^{-a} \phi(x_{-2}) \cos \frac{r\pi}{a}(x_{-2} + 2a)\, dx_{-2}\right.$$

$$+\int_{-a}^{0} \phi(x_{-1}) \cos \frac{r\pi}{a}(x_{-1} + a)\, dx_{-1} + \int_{0}^{a} \phi(x_0) \cos \frac{r\pi}{a} x_0\, dx_0$$

$$\left.+\int_{a}^{2a} \phi(x_1) \cos \frac{r\pi}{a}(x_1 - a)\, dx_1 + \int_{2a}^{3a} \phi(x_2) \cos \frac{r\pi}{a}(x_2 - 2a)\, dx_2 \ldots\right]$$

where $r = 2, 4, 6 \ldots$

or

$$b_r = \frac{2}{a}\int_{-\infty}^{\infty} \phi(x) \cos \frac{r\pi x}{a}\, dx \tag{37}$$

where $r = 2, 4, 6 \ldots$.

On substituting from equation (31), equations (36) and (37) become

$$\left.\begin{aligned} b_0 &= \frac{1}{a} \\ b_r &= \frac{2}{a} e^{-\frac{r\pi\delta}{a}} \end{aligned}\right\} \tag{38}$$

where $r = 2, 4, 6 \ldots$.

Next consider the infinitely long beam acted upon only by a continuous load of the type

$$\psi(x) = \ldots + \phi(x - 2a) - \phi(x - a) + \phi(x) - \phi(x + a) + \phi(x + 2a) \ldots \tag{39}$$

where as before $\phi(x)$ is a suitably restricted even function of x. The function $\psi(x)$ is an even function of period $2a$. Further, $\psi(x + a) = \psi(x - a) = -\psi(x)$. Consequently, $\psi(x)$ can be represented by the Fourier series

$$\psi(x) = b_1 \cos \frac{\pi x}{a} + b_3 \cos \frac{3\pi x}{a} + b_5 \cos \frac{5\pi x}{a} + \ldots \tag{40}$$

where

$$b_s = \frac{2}{a}\int_{0}^{a} \psi(x) \cos \frac{sx}{a}\, dx \qquad (s = 1, 3, 5 \ldots) \tag{41}$$

On substituting from equation (40), equation (41) becomes

$$b_s = \frac{2}{a}\left[\ldots + \int_0^a \phi(x - 2a)\cos\frac{s\pi x}{a}\,dx - \int_0^a \phi(x - a)\cos\frac{s\pi x}{a}\,dx\right.$$

$$\left. + \int_0^a \phi(x)\cos\frac{s\pi x}{a}\,dx - \int_0^a \phi(x + a)\cos\frac{s\pi x}{a}\,dx + \int_0^a \phi(x + 2a)\cos\frac{s\pi x}{a}\,dx \ldots\right]$$

where $s = 1, 3, 5 \ldots$.

By making use of equation (35), it follows that

$$b_s = \frac{2}{a}\left[\ldots + \int_{-2a}^{-a} \phi(x_{-2})\cos\frac{s\pi}{a}(x_{-2} + 2a)\,dx_{-2}\right.$$

$$- \int_{-a}^{0} \phi(x_{-1})\cos\frac{s\pi}{a}(x_{-1} + a)\,dx_{-1} + \int_0^a \phi(x_0)\cos\frac{s\pi x_0}{a}\,dx_0$$

$$\left. - \int_a^{2a} \phi(x_1)\cos\frac{s\pi}{a}(x_1 - a)\,dx_1 + \int_{2a}^{3a} \phi(x_2)\cos\frac{s\pi}{a}(x_2 - 2a)\,dx_2 \ldots\right]$$

where $s = 1, 3, 5 \ldots$

or

$$b_s = \frac{2}{a}\int_{-\infty}^{\infty} \phi(x)\cos\frac{s\pi x}{a}\,dx$$

where $s = 1, 3, 5 \ldots$.

By making use of expression (31) for $\phi(x)$, it follows that

$$b_s = \frac{2}{a}\, e^{-\frac{s\pi\delta}{a}} \tag{42}$$

where $s = 1, 3, 5 \ldots$ and δ is taken very small in the applications that follow.

Beam of Finite Length

It is now possible to investigate the main problems of this paper, that is, finite beams loaded in various ways and having either clamped or freely supported ends.

Take the load to consist of a series of isolated loads $-W$ on the upper face of the beam, with a series of equal and opposite supporting pressures on the lower face halfway between the loads, as shown in

figure 2(a). This distribution of forces may be resolved into the sum of the two distributions shown in figures 2(b) and 2(c), which are most conveniently treated separately.

In order to calculate the effect of the forces shown in figure 2(c), it follows on reference to equations (15), (30), and (38) that $m = \frac{r\pi}{a}$, and it is necessary to write

$$\left.\begin{aligned} H &= -\frac{W}{a} \\ \text{or} \qquad H &= -\frac{2W}{a} e^{-\frac{r\pi\delta}{a}} \end{aligned}\right\} \tag{43}$$

accordingly as $r = 0$ or $r > 0$ and sum for even values of r. Thus, the stress components are, in figure 2(c):

$$\left.\begin{aligned} Y_y &= \frac{W}{a}\left[-\frac{1}{2} + \sum_{r=2,\ldots}^{\infty} \frac{e^{-\frac{r\pi\delta}{a}}}{D_1}\left(\beta \sinh \frac{r\pi\beta\epsilon h}{a} \cosh \frac{r\pi\alpha\eta}{a}\right.\right. \\ &\qquad \left.\left. -\alpha \sinh \frac{r\pi\alpha\epsilon h}{a} \cosh \frac{r\pi\beta\eta}{a}\right) \cos \frac{r\pi x}{a}\right] \\ X_x &= -\frac{W\epsilon^2}{a} \sum_{r=2,\ldots}^{\infty} \frac{e^{-\frac{r\pi\delta}{a}}}{D_1}\left(\alpha \sinh \frac{r\pi\beta\epsilon h}{a} \cosh \frac{r\pi\alpha\eta}{a}\right. \\ &\qquad \left. -\beta \sinh \frac{r\pi\alpha\epsilon h}{a} \cosh \frac{r\pi\beta\eta}{a}\right) \cos \frac{r\pi x}{a} \\ X_y &= -\frac{W\epsilon}{a} \sum_{r=2,\ldots}^{\infty} \frac{e^{-\frac{r\pi\delta}{a}}}{D_1}\left(\sinh \frac{r\pi\beta\epsilon h}{a} \sinh \frac{r\pi\alpha\eta}{a}\right. \\ &\qquad \left. -\sinh \frac{r\pi\alpha\epsilon h}{a} \sinh \frac{r\pi\beta\eta}{a}\right) \sin \frac{r\pi x}{a} \end{aligned}\right\} \tag{44}$$

where r has even values and

$$D_1 = \alpha \sinh \frac{r\pi\alpha\epsilon h}{a} \cosh \frac{r\pi\beta\epsilon h}{a} - \beta \sinh \frac{r\pi\beta\epsilon h}{a} \cosh \frac{r\pi\alpha\epsilon h}{a} \tag{45}$$

In order to calculate the effect of the system of forces indicated in figure 2(b), it appears on reference to equations (27), (40), and (42) that it is necessary to write

$$H = \frac{-2W}{a} e^{-\frac{s\pi\delta}{a}}$$

$$m = \frac{s\pi}{a}$$

and sum for odd values of s. Thus, the stress components are, for the case shown in figure 2(b):

$$\left.\begin{aligned}
Y_y &= -\frac{W}{a}\sum_{s=1,\ldots}^{\infty}\frac{e^{-\frac{s\pi\delta}{a}}}{D_2}\left(\beta\cosh\frac{s\pi\beta\epsilon h}{a}\sinh\frac{s\pi\alpha\eta}{a}\right.\\
&\qquad\left.-\alpha\cosh\frac{s\pi\alpha\epsilon h}{a}\sinh\frac{s\pi\beta\eta}{a}\right)\cos\frac{s\pi x}{a}\\
X_x &= \frac{W\epsilon^2}{a}\sum_{s=1,\ldots}^{\infty}\frac{e^{-\frac{s\pi\delta}{a}}}{D_2}\left(\alpha\cosh\frac{s\pi\beta\epsilon h}{a}\sinh\frac{s\pi\alpha\eta}{a}\right.\\
&\qquad\left.-\beta\cosh\frac{s\pi\alpha\epsilon h}{a}\sinh\frac{s\pi\beta\eta}{a}\right)\cos\frac{s\pi x}{a}\\
X_y &= \frac{W\epsilon}{a}\sum_{s=1,\ldots}^{\infty}\frac{e^{-\frac{s\pi\delta}{a}}}{D_2}\left(\cosh\frac{s\pi\beta\epsilon h}{a}\cosh\frac{s\pi\alpha\eta}{a}\right.\\
&\qquad\left.-\cosh\frac{s\pi\alpha\epsilon h}{a}\cosh\frac{s\pi\beta\eta}{a}\right)\sin\frac{s\pi x}{a}
\end{aligned}\right\} \qquad (46)$$

where s has odd values and

$$D_2 = \beta\sinh\frac{s\pi\alpha\epsilon h}{a}\cosh\frac{s\pi\beta\epsilon h}{a} - \alpha\sinh\frac{s\pi\beta\epsilon h}{a}\cosh\frac{s\pi\alpha\epsilon h}{a} \qquad (47)$$

If now δ is taken to be very small, the sum of the two stress distributions (equations (44) and (46)) would give a stress distribution that very closely approximates one arising from a series of loads W distributed over small areas, as shown in figure 2(a). It is evident from figure 2(c) that the stress components given by equation (44) will be relatively unimportant except in the immediate neighborhood of the place of application of the forces.

It is now possible to draw some conclusions concerning the flexure of finite beams under concentrated loads. Consider the portion represented by OS in figure 3. It closely approximates a beam of length 2a clamped horizontally at the ends and carrying a load W at the center.

Again, consider the portion PR. This part closely approximates a beam of length a supported by vertical shearing forces of amount $\frac{1}{2}W$ on the two terminal sections, having zero bending moments at P and R

and carrying a load W at the center. Thus section PR represents approximately a beam of length a, simply supported at the ends and carrying a load W at the center.

A Simple Method for Computing Equations (44) and (46)

It is possible to express approximately each stress component given in equations (44) and (46) in two parts, each having a finite number of terms. The approximation can be made as close as desired. As an illustration of the method of transforming the expressions for the stress components in this manner, the process is carried through in detail for the stress component X_y given in equation (44). By dividing both numerator and denominator by $\cosh \frac{r\pi\alpha\epsilon h}{a} \cosh \frac{r\pi\beta\epsilon h}{a}$, it results that the stress component X_y in equation (44) becomes

$$X_y = -\frac{W\epsilon}{a} \sum_{r=2,\ldots}^{\infty} e^{-\frac{r\pi\delta}{a}} \left[\frac{\left(\tanh \frac{r\pi\beta\epsilon h}{a}\right) \frac{\sinh \frac{r\pi\alpha\eta}{a}}{\cosh \frac{r\pi\alpha\epsilon h}{a}} - \left(\tanh \frac{r\pi\alpha\epsilon h}{a}\right) \frac{\sinh \frac{r\pi\beta\eta}{a}}{\cosh \frac{r\pi\beta\epsilon h}{a}}}{\alpha \tanh \frac{r\pi\alpha\epsilon h}{a} - \beta \tanh \frac{r\pi\beta\epsilon h}{a}} \right] \sin \frac{r\pi x}{a}$$

where r has even values. It is evident that for all terms of this series in which r is greater than or equal to some number t, it is approximately correct to write

$$\tanh \frac{r\pi\beta\epsilon h}{a} = \tanh \frac{r\pi\alpha\epsilon h}{a} = 1$$

$$\cosh \frac{r\pi\beta\epsilon h}{a} = \frac{1}{2} e^{\frac{r\pi\beta\epsilon h}{a}}$$

$$\cosh \frac{r\pi\alpha\epsilon h}{a} = \frac{1}{2} e^{\frac{r\pi\alpha\epsilon h}{a}}$$

Hence, approximately

$$X_y = -\frac{W\epsilon}{a}\left\{\sum_{r=2}^{t-2} e^{-\frac{r\pi\delta}{a}}\left[\frac{\left(\tanh\frac{r\pi\beta\epsilon h}{a}\right)\frac{\sinh\frac{r\pi\alpha\eta}{a}}{\cosh\frac{r\pi\alpha\epsilon h}{a}} - \left(\tanh\frac{r\pi\alpha\epsilon h}{a}\right)\frac{\sinh\frac{r\pi\beta\eta}{a}}{\cosh\frac{r\pi\beta\epsilon h}{a}}}{\alpha\tanh\frac{r\pi\alpha\epsilon h}{a} - \beta\tanh\frac{r\pi\beta\epsilon h}{a}}\right]\sin\frac{r\pi x}{a}\right.$$

$$+\frac{1}{(\alpha-\beta)}\sum_{r=t}^{\infty} e^{-\frac{r\pi\delta}{a}}\left[e^{-\frac{r\pi\alpha\epsilon h}{a}}\left(e^{\frac{r\pi\alpha\eta}{a}} - e^{-\frac{r\pi\alpha\eta}{a}}\right)\right.$$

$$\left.\left. - e^{-\frac{r\pi\beta\epsilon h}{a}}\left(e^{\frac{r\pi\beta\eta}{a}} - e^{-\frac{r\pi\beta\eta}{a}}\right)\right]\sin\frac{r\pi x}{a}\right\} \qquad (48)$$

where the summation is of even values of r and t is an even number and chosen so that

$$\frac{t\pi\beta\epsilon h}{a} \geq 2.4 \qquad (49)$$

A closer approximation results if t is taken still larger than equation (49) would indicate. However, the approximation (equation (49)) appears to be reasonably good.

After writing in exponential form the trigonometric factor $\sin\frac{r\pi x}{a}$ occurring in the infinite series in equation (48), four infinite geometrical progressions are obtained, each of which is readily summed. It is found that

$$X_y = -\frac{W\epsilon}{a}\left(\sum_{r=2}^{t-2} e^{-\frac{r\pi\delta}{a}}\left(\frac{\sinh\frac{r\pi\beta\epsilon h}{a}\sinh\frac{r\pi\alpha\eta}{a} - \sinh\frac{r\pi\alpha\epsilon h}{a}\sinh\frac{r\pi\beta\eta}{a}}{\alpha\sinh\frac{r\pi\alpha\epsilon h}{a}\cosh\frac{r\pi\beta\epsilon h}{a} - \beta\sinh\frac{r\pi\beta\epsilon h}{a}\cosh\frac{r\pi\alpha\epsilon h}{a}}\right)\sin\frac{r\pi x}{a}\right.$$

$$+\frac{1}{(\alpha-\beta)}\left\{\frac{e^{t\gamma_1}\left[\sin t\lambda - e^{2\gamma_1}\sin(t-2)\lambda\right]}{1-2e^{2\gamma_1}\cos 2\lambda + e^{4\gamma_1}} + \frac{e^{-t\rho_1}\left[-\sin t\lambda + e^{-2\rho_1}\sin(t-2)\lambda\right]}{1-2e^{-2\rho_1}\cos 2\lambda + e^{-4\rho_1}}\right.$$

$$\left.\left.-\frac{e^{t\gamma_2}\left[\sin t\lambda - e^{2\gamma_2}\sin(t-2)\lambda\right]}{1-2e^{2\gamma_2}\cos 2\lambda + e^{4\gamma_2}} - \frac{e^{-t\rho_2}\left[-\sin t\lambda + e^{-2\rho_2}\sin(t-2)\lambda\right]}{1-2e^{-2\rho_2}\cos 2\lambda + e^{-4\rho_2}}\right\}\right) \qquad (50)$$

where

$$\left.\begin{aligned}\gamma_1 &= \frac{\pi}{a}\left[\alpha\epsilon\,(y-h) - \delta\right]\\ \gamma_2 &= \frac{\pi}{a}\left[\beta\epsilon\,(y-h) - \delta\right]\\ \rho_1 &= \frac{\pi}{a}\left[\alpha\epsilon\,(y+h) + \delta\right]\\ \rho_2 &= \frac{\pi}{a}\left[\beta\epsilon\,(y+h) + \delta\right]\\ \lambda &= \frac{\pi x}{a}\end{aligned}\right\} \qquad (51)$$

Usually, it is not necessary to take t larger than 12 or 14. However, in each case equation (49) must be used in order to establish the value of t needed.

By applying this method to the other stress components and rewriting the expression for X_y, it results that equation (44) can be written approximately as

$$
\left.
\begin{aligned}
Y_y &= \frac{W}{a}\left\{ -\frac{1}{2} + \sum_{r=2}^{t-2} \frac{e^{-\frac{r\pi\delta}{a}}}{D_1}\left(\beta \sinh r\nu_2 h \cosh r\nu_1 y - \alpha \sinh r\nu_1 h \cosh r\nu_2 y\right) \cos\frac{r\pi x}{a} \right.\\
&\qquad \left. + R\left[\beta f(t,\gamma_1) + \beta f(t,-\rho_1) - \alpha f(t,\gamma_2) - \alpha f(t,-\gamma_2)\right]\right\}\\
X_x &= -\frac{W\epsilon^2}{a}\left\{ \sum_{r=2}^{t-2} \frac{e^{-\frac{r\pi\delta}{a}}}{D_1}\left(\alpha \sinh r\nu_2 h \cosh r\nu_1 y - \beta \sinh r\nu_1 h \cosh r\nu_2 y\right) \cos\frac{r\pi x}{a} \right.\\
&\qquad \left. + R\left[\alpha f(t,\gamma_1) + \alpha f(t,-\rho_1) - \beta f(t,\gamma_2) - \beta f(t,-\rho_2)\right]\right\}\\
X_y &= -\frac{W\epsilon}{a}\left\{ \sum_{r=2}^{t-2} \frac{e^{-\frac{r\pi\delta}{a}}}{D_1}\left(\sinh r\nu_2 h \sinh r\nu_1 y - \sinh r\nu_1 h \sinh r\nu_2 y\right) \sin\frac{r\pi x}{a} \right.\\
&\qquad \left. + R\left[-if(t,\gamma_1) + if(t,-\rho_1) + if(t,\gamma_2) - if(t,-\rho_2)\right]\right\}
\end{aligned}
\right\} \tag{52}
$$

where

$$
\left.
\begin{aligned}
\nu_1 &= \frac{\pi\alpha\epsilon}{a}\\
\nu_2 &= \frac{\pi\beta\epsilon}{a}\\
t &\geq \frac{2.4}{\nu_2 h} \quad (t \text{ even})\\
f(p,q) &= \frac{e^{p(q+i\lambda)}\left[1 - e^{2(q-i\lambda)}\right]}{(\alpha-\beta)\left[1 - 2e^{2q}\cos 2\lambda + e^{4q}\right]}
\end{aligned}
\right\} \tag{53}
$$

$i = \sqrt{-1}$; D_1, D_2, γ_1, γ_2, ρ_1, ρ_2, and λ are given by equations (45), (47), and (51); and R means that the real part of the expression following it is to be taken. Correspondingly, equation (46) can be written approximately as

$$
\left.
\begin{aligned}
Y_y &= -\frac{W}{a}\left\{\sum_{s=1}^{m-2} \frac{e^{-\frac{s\pi\delta}{a}}}{D_2}\left(\beta \cosh s\nu_2 h \sinh s\nu_1 y - \alpha \cosh s\nu_1 h \sinh s\nu_2 y\right) \cos\frac{s\pi x}{a}\right.\\
&\qquad \left. + R\left[-\beta f(m, \gamma_1) + \beta f(m, -\rho_1) + \alpha f(m, \gamma_2) - \alpha f(m, -\rho_2)\right]\right\}\\
X_x &= \frac{W\epsilon^2}{a}\left\{\sum_{s=1}^{m-2} \frac{e^{-\frac{s\pi\delta}{a}}}{D_2}\left(\alpha \cosh s\nu_2 h \sinh s\nu_1 y - \beta \cosh s\nu_1 h \sinh s\nu_2 y\right) \cos\frac{s\pi x}{a}\right.\\
&\qquad \left. + R\left[-\alpha f(m, \gamma_1) + \alpha f(m, -\rho_1) + \beta f(m, \gamma_2) - \beta f(m, -\rho_2)\right]\right\}\\
X_y &= \frac{W\epsilon}{a}\left\{\sum_{s=1}^{m-2} \frac{e^{-\frac{s\pi\delta}{a}}}{D_2}\left(\cosh s\nu_2 h \cosh s\nu_1 y - \cosh s\nu_1 h \cosh s\nu_2 y\right) \sin\frac{s\pi x}{a}\right.\\
&\qquad \left. + R\left[i f(m, \gamma_1) + i f(m, -\rho_1) - i f(m, \gamma_2) - i f(m, -\rho_2)\right]\right\}
\end{aligned}
\right\} \quad (54)
$$

where s is odd; $m \geq \frac{2.4}{\nu_2 h}$ when m is odd; D_1, D_2, γ_1, γ_2, ρ_1, ρ_2, λ, f, and i are given as before by equations (45), (47), (51), and (53); and R means that the real part of the expression following it is to be taken.

It is to be remembered that equation (52) for a small value of δ gives the stress components corresponding to the load distribution shown in figure 2(c), except that the loads are distributed over a small area. The results for point loads are obtained by setting δ equal to zero. (84 percent of the area under the curve of equation (31) is over a length 2δ on either side of $x = 0$.) Similarly, equation (54) corresponds to the load

distribution shown in figure 2(b). Neither of these load distributions alone would be of much practical importance. However, by adding the two distributions, the resulting stress distribution is that of an infinite beam loaded at equal intervals by equal concentrated forces acting in the upward and downward directions alternately, as shown by figure 2(a). From the combined stress distribution, it is possible to draw some conclusions regarding beams of finite length subjected to concentrated loading.

Reduction of Equations (52) and (54) for an Isotropic Beam

The stress components given in equations (52) and (54) admit some simplification when they are applied to an isotropic beam. Although the isotropic case is not being considered in this report, it may be of interest to determine the forms to which equations (52) and (54) reduce in this case. For the isotropic case, β approaches α as α' approaches 1, and ϵ also becomes equal to 1. For these values of α and β, equations (52) and (54) become indeterminate. By evaluating (noting that ν, ν_2, γ, γ_2, ρ_1, and ρ_2 are functions of α and β), it results that for an isotropic beam, equation (52) becomes

$$
\left.
\begin{aligned}
Y_y &= \frac{W}{a}\left\{-\frac{1}{2} + \sum_{r=2}^{t-2} \frac{e^{-\frac{r\pi\delta}{a}}}{\Delta_1}\left[\sinh\frac{r\pi h}{a}\left(\frac{r\pi y}{a}\sinh\frac{r\pi y}{a} - \cosh\frac{r\pi y}{a}\right)\right.\right.\\
&\quad \left.\left. - \frac{r\pi h}{a}\cosh\frac{r\pi h}{a}\cosh\frac{r\pi y}{a}\right]\cos\frac{r\pi x}{a}\right.\\
&\quad \left. + R\left[\frac{\pi}{a}(y-h)P(t,\gamma) - \frac{\pi}{a}(y+h)P(t,-\rho) - f(t,\gamma) - f(t,-\rho)\right]\right\}\\
X_x &= -\frac{W}{a}\left\{\sum_{r=2}^{t-2} \frac{e^{-\frac{r\pi\delta}{a}}}{\Delta_1}\left[\sinh\frac{r\pi h}{a}\left(\frac{r\pi y}{a}\sinh\frac{r\pi y}{a} + \cosh\frac{r\pi y}{a}\right)\right.\right.\\
&\quad \left.\left. - \frac{r\pi h}{a}\cosh\frac{r\pi h}{a}\cosh\frac{r\pi y}{a}\right]\cos\frac{r\pi x}{a}\right.\\
&\quad \left. + R\left[\frac{\pi}{a}(y-h)P(t,\gamma) - \frac{\pi}{a}(y+h)P(t,-\rho) + f(t,\gamma) + f(t,-\rho)\right]\right\}\\
X_y &= -\frac{W}{a}\left\{\sum_{r=2}^{t-2} \frac{e^{-\frac{r\pi\delta}{a}}}{\Delta_1}\left(\frac{r\pi y}{a}\sinh\frac{r\pi h}{a}\cosh\frac{r\pi y}{a}\right.\right.\\
&\quad \left.\left. - \frac{r\pi h}{a}\cosh\frac{r\pi h}{a}\sinh\frac{r\pi y}{a}\right)\sin\frac{r\pi x}{a}\right.\\
&\quad \left. + R\left[-\frac{i\pi}{a}(y-h)P(t,\gamma) - \frac{i\pi}{a}(y+h)P(t,-\rho)\right]\right\}
\end{aligned}
\right\} \quad (55)
$$

where r is even and

$$t \geq \frac{3.5a}{\pi h} \text{ (t even)}, \quad \lambda = \frac{\pi x}{a}, \quad \gamma = \frac{\pi}{a}\left[(y - h) - \delta\right], \quad \rho = \frac{\pi}{a}\left[(y + h) + \delta\right]$$

$$P(p,q) = \frac{e^{p(q+i\lambda)}}{\left(1 - 2e^{2q}\cos 2\lambda + e^{4q}\right)^2}\left[p - 2(p-2)e^{2q}\cos 2\lambda + (p-4)e^{4q} - (p+2)e^{2(q-i\lambda)} + 2pe^{2(2q-i\lambda)}\cos 2\lambda - (p-2)e^{2(3q-i\lambda)}\right]$$

$$f(p, q) = \frac{e^{p(q+i\lambda)}\left[1 - e^{2(q-i\lambda)}\right]}{(\alpha - \beta)\left(1 - 2e^{2q}\cos 2\lambda + e^{4q}\right)} \qquad (56)$$

$$i = \sqrt{-1}$$

$$\Delta_1 = \frac{r\pi h}{a} + \sinh\frac{r\pi h}{a}\cosh\frac{r\pi h}{a}$$

and R means that the real part of the expression following it is to be taken. A closer approximation to the actual stress component in the isotropic case results the larger the value of t is taken. However, any value of $t > \frac{3.5a}{\pi h}$ appears from numerous computations to be reasonably satisfactory. Similarly, equation (55) becomes for an isotropic beam:

$$
\left.
\begin{aligned}
Y_y = -\frac{W}{a}\Bigg\{ & \sum_{s=1}^{m-2} \frac{e^{-\frac{s\pi\delta}{a}}}{\Delta_2}\left[\cosh\frac{s\pi h}{a}\left(\frac{s\pi y}{a}\cosh\frac{s\pi y}{a}-\sinh\frac{s\pi y}{a}\right)\right. \\
& \left. -\frac{s\pi h}{a}\sinh\frac{s\pi h}{a}\sinh\frac{s\pi y}{a}\right]\cos\frac{s\pi x}{a} \\
& + R\left[-\frac{\pi}{a}(y-h)\,P(m,\gamma)-\frac{\pi}{a}(y+h)\,P(m,-\rho)+f(m,\gamma)-f(m,-\rho)\right]\Bigg\} \\
X_x = \frac{W}{a}\Bigg\{ & \sum_{s=1}^{m-2} \frac{e^{-\frac{s\pi\delta}{a}}}{\Delta_2}\left[\cosh\frac{s\pi h}{a}\left(\frac{s\pi y}{a}\cosh\frac{s\pi y}{a}+\sinh\frac{s\pi y}{a}\right)\right. \\
& \left. -\frac{s\pi h}{a}\sinh\frac{s\pi h}{a}\sinh\frac{s\pi y}{a}\right]\cos\frac{s\pi x}{a} \\
& + R\left[-\frac{\pi}{a}(y-h)\,P(m,\gamma)-\frac{\pi}{a}(y+h)\,P(m,-\rho)-f(m,\gamma)+f(m,-\rho)\right]\Bigg\} \\
X_y = \frac{W}{a}\Bigg\{ & \sum_{s=1}^{m-2} \frac{e^{-\frac{s\pi\delta}{a}}}{\Delta_2}\left[\frac{s\pi y}{a}\cosh\frac{s\pi h}{a}\sinh\frac{s\pi y}{a}\right. \\
& \left. -\frac{s\pi h}{a}\sinh\frac{s\pi h}{a}\cosh\frac{s\pi y}{a}\right]\sin\frac{s\pi x}{a} \\
& + R\left[i\frac{\pi}{a}(y-h)\,P(m,\gamma)-i\frac{\pi}{a}(y+h)\,P(m,-\rho)\right]\Bigg\}
\end{aligned}
\right\} \quad (57)
$$

where

$$m \geq \frac{3.5a}{h} \text{ (odd)}$$

$$\Delta_2 = \frac{s\pi h}{a} - \sinh\frac{s\pi h}{a}\cosh\frac{s\pi h}{a}$$

s is odd; γ, ρ, λ, P, f, and i are given by equation (56); and R means again that the real part of the expression following it is to be used.

EXPERIMENTAL VERIFICATION OF ANALYSIS

In the vicinity of a concentrated load on a beam, the distribution of the longitudinal shear over a cross section is markedly different from that predicted by the elementary theory. An estimate of the accuracy of the method can be obtained by a comparison of an experimental determination of this distribution with that calculated by the mathematical method described herein. Such an experimental determination and a comparison were made and are described in the following sections.

Description of Test

The plan was, broadly, to obtain a solid wood beam of uniform structure, to fix 47 metalectric gages on each face in the vicinity of the load point, to apply load and record strains by means of metalectric rosettes by using a 48-point recorder connected first to the gages on one face with one check gage on the other face, and then to repeat the application of load in identical manner and record strains by using the recorder connected to the gages on the opposite faces.

A clear, straight-grained Sitka spruce beam was selected. The rough piece was 3 inches by 10 inches by 16 feet with the 10-inch dimension in the tangential direction. The annual rings numbered about 18 to the inch and their radius of curvature was approximately 3 feet. The grain was almost parallel to the length of the beam throughout. One-half the rough piece was surfaced on four sides and trimmed on the ends to give a finished beam 1.99 by 9.37 by 96.03 inches. The specimen was then stored in a room of constant temperature and humidity for 3 weeks until its weight became constant.

It was desirable to obtain strains in three directions at definite points on the surfaces of the beam. The use of electric-resistance-type strain gages appeared most feasible provided that a short enough gage length can be obtained. Metalectric gages with $\frac{1}{8}$-inch and $\frac{1}{4}$-inch gage lengths and rosettes with 1-inch gage lengths are commercially available. Strains measured by these gages are average strains over the gage length, and, therefore, the 1-inch rosettes are not suitable for the purpose. Rosettes can be built up, with either the $\frac{1}{8}$- or $\frac{1}{4}$-inch gages, by mounting the gages on top of each other. The $\frac{1}{8}$-inch gages are 1/4 inch wide, so that when they are superimposed on each other, the first gage is shorter than the width of the gage beneath it. This was believed to be undesirable, and the $\frac{1}{8}$-inch gages were, therefore, not employed. The $\frac{1}{4}$-inch gages were 1/8 inch wide and, therefore, this difficulty was not encountered in their use. Rosettes were built up of these gages, and the effect of superimposing the individual gages on each other was found as follows.

Three rosettes, built of three gages each, were mounted on the center line of a strip of clear Sitka spruce 1/4 inch thick, 1 inch wide, and about 24 inches long, which was then subjected to tension. The positions of the gages are shown in figure 4, and the values of the strains observed for a series of loads are given in table 1. In rosette A, the longitudinal gage is applied directly on the wood. In rosette B, the longitudinal gage is between the other two gages. In rosette C, the longitudinal gage is superimposed on both of the other two gages.

Examination of the data tabulated in table 1 shows that the strain readings were duplicated to within 0.00002 inch per inch in successive loadings. The charts from the recorder were read accurately to about 0.000008 inch per inch. Higher accuracy was not possible because of the thickness of the recording trace. When the traces overlapped prior traces, the readings were less accurate.

The data also indicate that the position of the gage in the rosette does not significantly influence the strain recorded. The longitudinal strain measured by gage 1 in rosette A (fig. 4) can be assumed to be correct because the gage was mounted directly on the wood. Strains measured by gage 2 of rosette B, which was superimposed on one other gage, showed increases compared with gage 1 of 0.000010 inch per inch in the first and 0.000016 inch per inch in the second loading at a load of 750 pounds. The longitudinal strains measured by gage 3 of rosette C at the same successive loads were 0.000060 and 0.000068 inch per inch greater than those measured by gage 1. Thus these data indicate that the superimposed longitudinal gages undergo greater strains than the gage mounted directly on the wood. However, the gages measuring strain at 45° to the longitudinal direction do not confirm this indication. Gage 6 was applied directly on the wood. Gage 4, which was applied on one other gage, yielded values of strain 0.000040 and 0.000050 inch per inch less than those of gage 6; and gage 5, which was superimposed on two other gages, yielded values 0.000050 and 0.000040 inch per inch less than those of gage 6. Gage 8 was also applied directly on the wood. Gage 9, which was superimposed on one other gage, yielded values 0.000060 inch per inch less than that of gage 8; and gage 7, which was superimposed on two other gages, yielded values 0.000030 inch per inch greater than the value of gage 8. These results indicate that the position of a gage (bottom, center, or top) in a built-up rosette apparently has no consistent effect on the recorded strains. Furthermore, the differences in the magnitudes of the strains read by gages oriented in the same direction are so small that they might very well be differences in actual strain from point to point in the specimen. It is assumed, therefore, that rosettes of this type yield values of strain that are sufficiently accurate for the purpose of this report.

Gages of this type were mounted on the beam while it was approaching its equilibrium moisture content in the humidity room. Their positions are shown by the sketch (fig. 5) and by the coordinates in table 2. The rosettes were built up with the gage measuring strain in the longitudinal direction of the beam applied directly to the wood and centered on the point shown in figure 5. The gage measuring strain at 90° to the longitudinal direction was superimposed on the first gage and centered on the same point. The third gage, which measured strain at 45° to the longitudinal, was superimposed on the first two gages and centered on the same point. Additional gages with 1-inch gage length were applied to measure longitudinal strains in the vicinity of the neutral axis as shown.

Points symmetrically arranged about the line of action of the load were accurately laid out on both faces of the beam by using a square and a scale graduated to 0.01 inch. Application of the gages required that a prime coating of glue be allowed to dry on the wood. Fresh glue was spread on both the gage and the beam, and then the gage was firmly pressed into position, the squeezed-out glue was removed, and a weighted piece of sponge rubber to apply pressure was left on the gage for 48 hours. The layout lines were covered by the first gage applied, so that the lines were redrawn on top of the gage for applying the superimposed gage. However, after all gages were applied and the coordinates were measured for the center of each gage, it was observed that some individual gages were centered as much as 0.04 inch from the point desired. In comparison with the dimensions of the beam, the location of gages was considered satisfactory and was within 0.03 inch of the average values given in table 2.

The beam was tested in the room of controlled temperature and humidity after equilibrium moisture content was attained. A four-screw mechanical testing machine of 10,000-pound capacity was used with a static-bending jig centered on the weighing platform. The jig was made of a pair of 4-inch I-beams bolted together with spacers to give a $\frac{3}{4}$-inch clearance between flanges. Laterally adjustable supports were spaced symmetrically from the center of the jig to give a 6-foot span and were bolted to the top flanges. The beam was then centered on the supports, and roller-bearing plates were inserted between the beam and the laterally adjustable supports. Load was applied to the center of the beam by means of a spherical head and a hard-maple bearing block cut in the shape of a cylindrical segment.

A great amount of difficulty was encountered in attempts to apply the load. Several loading blocks were each tried in several preliminary loadings, but the observed values of strain were far from symmetrical about the plane in which load was applied. The slightest change in the position of the loading block produced large change in the strains on the faces of the beam. Consecutive loadings under conditions reproduced as closely as possible for each load did not produce identical strains. The plan to observe strains in each face of the beam in two consecutive loadings was therefore discarded. The 1-inch gages in the vicinity of the neutral axis could not be read with sufficient accuracy to yield useful data; 48 gages were, therefore, selected for measurement of strain during a single application of the load. These gages are shown in circles in figure 5.

Before the final data were taken, a jointer cut 0.05 inch deep was taken along the top of the beam to remove any material that could have been overstressed beneath the load block during the previous applications of load. A new hard-maple load block was turned in a wood lathe to an 11-inch radius to insure a true cylindrical segment. The beam was again set up and small loads, less than 200 pounds, were applied to check the centering of the loading block against the symmetry of the gage readings.

Movements of 0.01 inch of the loading block were sufficient to produce definitely nonsymmetrical distributions of strain. When the loading block was centered to give approximately symmetrical strains, the beam was tested as follows.

The 48-point recorder was adjusted for the initial reading of each gage while a load of 15 pounds was maintained on the beam. Strains were then recorded for gages on both faces of the beam while consecutive loads of 100, 200, 300, 400, 500, and 600 pounds were maintained.

Observed strains were recorded while a constant deflection was maintained on the beam. Because the load was comparatively small and only a few minutes were required to record the strains, plastic flow of the material of the beam probably did not influence the strains observed. Certain gages registered such small increments of strain (less than 0.000008 in./in.) that the recorded traces overlapped and made accurate interpolation of the strain difficult. The readings taken for small increments of strain are, therefore, not so reliable as those taken for large increments.

After the beam was tested, specimens for the determination of its elastic properties were cut from it. They were taken from the central part of the beam. For the plate-shear test, these specimens consisted of two specimens measuring 1/4 by $9\frac{1}{4}$ by $9\frac{1}{4}$ inches each; and for the compression test, the specimens consisted of two specimens parallel to the grain and measuring 2 by 2 by 8 inches each and two specimens perpendicular to the grain and parallel to the depth of the beam and measuring 2 by 2 by 8 inches each.

From the static bending tests the modulus of elasticity only was determined. The modulus of rigidity in planes parallel to the faces of the beams was determined by the plate-shear tests. Modulus of elasticity in compression and Poisson's ratios in the TR-, TL-, LT-, and LR-directions were obtained by the compression tests.

Presentation of Data

Data obtained from the test of the beam are recorded in table 3. In column (1) are listed the west- and east-face gages shown in figure 5. The gage readings at 15, 100, 200, 300, 400, 500, and 600 pounds are given in columns (2) to (8), respectively. Dimensions of the beam at time of test were 1.99 by 9.32 by 96.03 inches. The strains tabulated were read and checked from the chart plotted by the 48-point strain recorder.

Readings of each gage are plotted in figure 6 and are grouped in accordance with distance from the plane in which the load was applied and with distance from the center line of the beam. The slope of these curves from 0 to 500 pounds was used to determine the strains tabulated in

column (9) of table 3. From these strains the shear strains in the xy-plane were computed for the points at which rosettes were located. In table 2 the x- and y- coordinates of the gages are given in columns 2, 3, 6, and 7, and the shear strains are tabulated in columns (4) and (8). The strains in both faces and at points 0.4 inch on each side of the load were averaged for each group of gage positions at symmetrical locations. These average values are given at the end of table 2.

Shear strains in the xy-plane of the beam when subjected to a 500-pound load were computed by the mathematical method previously presented for points 0.4 inch from the plane in which load was applied. Computations were based on the elastic properties given in table 4 obtained by tests of coupons cut from the beam after test. The strains were calculated for three distributions of load (δ equal to 0, 0.125, and 0.250 inch) by obtaining the shear stresses X_y from the third part of equations (52) and (54) and dividing their sum by the modulus of rigidity. This method of obtaining shear strains from shear stresses is valid only when the strains associated with the grain direction and the radial or tangential direction are required. (See references 8 and 9.)

For example, the strain computed at $x = 0.40$ and $y = 1.48$ with $\delta = 0$ was obtained as follows. First the value of $\frac{\epsilon}{a}$ was found from equation (4) to be 0.03594, and from equation (49) the value of t was established as 8. Then from equation (52) the term

$$-\frac{\epsilon}{a}\sum_{r=2}^{t-2}\frac{e^{-\frac{r\pi\delta}{a}}}{D_1}\left(\sinh r\nu_2 h \sinh r\nu_1 y - \sinh r\nu_1 h \sinh r\nu_2 y\right)\sin\frac{r\pi x}{a}$$

was evaluated and found to be 0.001002. The real part of the term

$$-\frac{\epsilon}{a}R\left[-if(t, \gamma_1) + if(t, -\rho_1) + if(t, \gamma_2) - if(t, -\rho_2)\right]$$

of equation (52) was found to be 0.002806. By adding these terms and multiplying by W the stress X_y was found equal to 0.003808W. In a similar manner for equation (54), m was first established equal to 7. The term

$$\frac{\epsilon}{a}\sum_{s=1}^{m-2}\frac{e^{-\frac{s\pi\delta}{a}}}{D_2}\left(\cosh s\nu_2 h \cosh s\nu_1 y - \cosh s\nu_1 h \cosh s\nu_2 y\right)\sin\frac{s\pi x}{a}$$

and the term

$$\frac{\epsilon}{a}R\left[if(m, \gamma_1) + if(m, -\rho_1) - if(m, \gamma_2) - if(m, -\rho_2)\right]$$

were found to be 0.004437 and 0.003925, respectively. On summing and multiplying by W, the value of X_y from equation (54) was found equal to 0.008362W. The sum of the stresses computed by equations (52) and (54)

gave the total shear stress X_y at the point equal to 0.01217W. By substituting the load per inch of width (500 lb/1.99 in.) for W and dividing by the modulus of rigidity μ_{xy}, the strain e_{xy} was found equal to 33.72×10^{-6}.

Computed strains for several points are given in table 5 in which columns (1) and (2) give the x- and y-coordinates of the points and columns (3), (4), and (5) give the strains, respectively, with δ equal to 0, 0.125, and 0.250 inch.

A comparison of the computed and the observed distribution of shear strains is presented in figure 7 in which three curves, one for each value of δ, and the average observed strains are plotted with distance from longitudinal center line as ordinate and the strains at points 0.4 inch from the plane of loading as abscissa.

RESULTS

The results of the computations given in table 5 and the average results of the tests given in table 2 are plotted in figure 7. In this figure the ordinates are distances upward from the center line of the beam and the abscissas are shear strain. The distribution of strain obtained by the elementary theory is also shown. The difference between the two methods is marked; that is, the method developed herein exhibits a high-stress concentration near the top of the beam and the elementary method yields a low maximum at the center of the beam.

The data from the test exhibit a stress concentration similar to that obtained by the more accurate theory. The measured strains at the two points 1.48 and 2.72 inches from the center of the beam agree with the theory within the accuracy of the experiment. The strains at these two points are so small that the corresponding traces on the chart of the recorder overlapped and could not be accurately read. The strain at 3.72 inches from the center of the beam agrees very well with the curve for $\delta = 0$ that is for a concentrated load. Of course, the load was not concentrated in the test but was applied over a length of about 0.4 inch by the cylindrical load block. However, at a distance from the region over which the load is applied the difference in the effect of a truly concentrated load and one applied over a small region should be small. The strain at 4.48 inches from the center of the beam shows the effect of the distribution of the load. At this point, the theory approximately agrees with experiments if δ is given the value of 0.250 inch. The strain is considerably less than that due to a concentrated load.

If the actual distribution of the load on the beam were known, a more accurate solution for the strain distribution near the load could be obtained by integrating the solution for a concentrated load of varying intensity over the loaded part of the beam. However, this distribution

is difficult to determine and usually is not known, and, therefore, further refinement of the method seems futile.

CONCLUDING REMARK

It appears that the shear strains computed by a derived mathematical method were verified, as closely as could be expected, by experiment on a wood beam of rectangular cross section.

Forest Products Laboratory, Forest Service
U. S. Department of Agriculture
Madison, Wis., February 18, 1947

REFERENCES

1. March, H. W.: Summary of Formulas for Flat Plates of Plywood under Uniform or Concentrated Loads. Mimeo. No. 1300, Forest Products Lab., U. S. Dept. Agriculture, Oct. 1941.

2. March, H. W.: Flat Plates of Plywood under Uniform or Concentrated Loads. Mimeo. No. 1312, Forest Products Lab., U. S. Dept. Agriculture, March 1942.

3. March, H. W.: Buckling of Flat Plywood Plates in Compression, Shear, or Combined Compression and Shear. Mimeo. No. 1316, Forest Products Lab., U. S. Dept. Agriculture, April 1942.

4. Filon, L. N. G.: On the Approximate Solution for the Bending of a Beam of Rectangular Cross-Section under Any System of Load, with Special Reference to Points of Concentrated or Discontinuous Loading. Phil. Trans. Roy. Soc. (London), ser. A, vol. 201, Aug. 1903, pp. 63-155.

5. Lamb, H.: Flexure of a Narrow Beam. Atti IV Cong. Intern. Matemat. (Rome), vol. 3, 1909, p. 12.

6. Smith, C. B.: Effect of Elliptic or Circular Holes on the Stress Distribution in Plates of Wood or Plywood Considered as Orthotropic Materials. Mimeo. No. 1510, Forest Products Lab., U. S. Dept. Agriculture, May 1944.

7. Love, A. E. H.: A Treatise on the Mathematical Theory of Elasticity. Fourth ed., Dover Pub. (New York), 1944.

8. Norris, C. B.: The Application of Mohr's Stress and Strain Circles to Wood and Plywood. Mimeo. No. 1317, Forest Products Lab., U. S. Dept. Agriculture, Feb. 1943.

9. March, H. W.: Stress-Strain Relations in Wood and Plywood Considered as Orthotropic Materials. Mimeo. No. 1503, Forest Products Lab., U. S. Dept. Agriculture, Feb. 1944.

TABLE 1.- STRAINS OBSERVED IN ROSETTES MOUNTED ON A STRIP OF WOOD SUBJECTED TO A TENSILE LOAD

Load (lb)	Strain (in./in.)								
	Gage 1	Gage 2	Gage 3	Gage 4	Gage 5	Gage 6	Gage 7	Gage 8	Gage 9
Second application of load									
50	0	0	0	0	0	0	0	0	0
100	108×10^{-6}	100×10^{-6}	112×10^{-6}	20×10^{-6}	10×10^{-6}	10×10^{-6}	60×10^{-6}	60×10^{-6}	50×10^{-6}
150	216	212	224	40	30	30	120	110	100
200	328	328	336	50	50	50	170	160	150
250	448	448	456	60	60	60	210	200	180
300	564	564	576	80	80	90	270	250	230
350	680	684	700	100	100	110	320	300	270
400	800	796	812	120	120	130	370	340	300
450	904	916	936	130	130	140	410	390	350
500	1032	1036	1060	160	160	170	470	430	390
550	1148	1160	1184	170	180	190	510	480	430
600	1268	1280	1312	190	200	220	560	530	480
650	1392	1400	1440	200	210	240	600	570	520
700	1516	1524	1548	220	230	270	650	530	570
750	1640	1656	1708	240	250	290	700	670	610
First application of load									
50	0	0	0	0	0	0	0	0	0
100	----	100	100	20	10	10	40	40	40
150	----	210	220	40	20	20	100	90	90
200	----	320	330	50	40	50	150	150	140
250	----	450	450	80	60	60	210	190	180
300	----	570	570	80	80	90	260	250	230
350	----	690	690	100	100	110	300	300	270
400	----	810	810	120	120	130	350	340	310
450	----	910	930	150	130	150	420	390	350
500	1030	1050	1060	170	150	170	470	430	390
550	1160	1170	1180	190	170	190	520	470	430
600	1270	1290	1310	200	190	210	560	520	480
650	1400	1410	1440	220	210	240	610	560	520
700	1520	1520	1560	240	230	260	650	610	560
750	1640	1650	1700	260	250	300	700	670	610

TABLE 2.- OBSERVED STRAINS, AVERAGE VALUES, AND COORDINATES FOR POINTS AT WHICH GAGES WERE LOCATED ON BEAM TESTED (AXES SHOWN IN FIG. 1)

Gage	Coordinates		Shear strain, e_{xy} (in./in.)	Gage	Coordinates		Shear strain, e_{xy} (in./in.)
	x (in.)	y (in.)			x (in.)	y (in.)	
(1)	(2)	(3)	(4)	(5)	(6)	(7)	(8)
West face				East Face			
1, 2, 3	0.97	4.48	442 x 10^{-6}	1, 2, 3	-1.03	4.48	-426 x 10^{-6}
4, 5, 6	.38	4.49	1140	4, 5, 6	-.40	4.43	-1400
7, 8, 9	-.40	4.48	-914	7, 8, 9	.40	4.47	946
10, 11, 12	-1.01	4.48	-314	10, 11, 12	-.40	3.72	-316
13, 14, 15	.37	3.71	376	13, 14, 15	.41	3.73	338
16, 17, 18	-.40	3.72	-260	16, 17, 18	.40	2.72	----
19, 20, 21	.37	2.72	50	19, 20, 21	-.40	1.48	-50
22, 23, 24	-.40	2.73	-58	22	.99	.23	----
25, 26, 27	.38	1.48	----	23	.99	.00	----
28, 29, 30	-.40	1.48	-36	24	1.00	-.19	----
31	5.01	.02	----	25	.01	.22	----
32	5.01	.21	----	26	-.01	-.17	----
33	5.00	-.17	----	27	.01	.39	----
34	.94	.22	----	28	.00	.01	----
35	.95	-.17	----	29	-1.04	.21	----
36	.94	.02	----	30	-1.03	.00	----
37	-.03	.23	----	31	-1.04	-.17	----
38	-.03	-.17	----	32	.00	4.48	----
39	-.04	.38	----	Top of beam		4.66	----
40	-.04	.03	----				
41	-1.04	-.17	----				
42	-1.05	.23	----				
43	-1.05	.03	----	Average values (both faces)	±0.40	4.48	1100
44	-5.00	.23	----		± .40	3.72	322
45	-4.99	.02	----		± .40	2.72	54
46	-5.00	-.17	----		± .40	1.48	43
47	-.03	4.48	----				
Top of beam		4.66	----				

TABLE 3.- LOAD-STRAIN DATA OBTAINED IN FINAL TEST OF BEAM

Gage	Gage readings (in./in.)							Strain increment from 0 to 500 lb (in./in.)
	15-lb load	100-lb load	200-lb load	300-lb load	400-lb load	500-lb load	600-lb load	
(1)	(2)	(3)	(4)	(5)	(6)	(7)	(8)	(9)
1W	582×20^{-6}	560×20^{-6}	536×20^{-6}	505×20^{-6}	479×20^{-6}	452×20^{-6}	432×20^{-6}	-272×10^{-6}
2W	339	340	341	341	342	342	342	6
3W	339	341	350	360	370	381	384	88
4W	585	570	553	537	520	505	499	-170
5W	935	896	832	767	700	625	553	-670
6W	632	642	655	673	686	700	699	150
7W	550	544	534	528	527	528	532	-24
8W	960	934	878	810	720	615	495	-748
9W	646	660	675	685	690	698	698	76
10W	780	760	725	702	678	648	615	-274
11W	575	577	577	575	575	573	573	0
12W	427	428	429	430	430	438	441	20
13W	587	580	573	570	566	562	554	-40
14W	1000	970	915	863	812	763	720	-696
15W	747	735	718	699	681	661	647	-180
16W	682	678	671	667	660	654	648	-52
17W	79?	761	707	660	610	540	520	-480
18W	735	728	710	700	686	672	660	-136
19W	684	679	672	664	660	652	647	-64
20W	700	685	662	640	620	600	580	-210
21W	642	635	620	612	600	589	578	-112
22W	582	578	568	562	556	550	542	-70
23W	908	892	862	840	818	790	770	-244
24W	840	836	815	805	790	778.	762	-128
19E	590	588	585	583	582	581	581	-18
20E	635	616	598	580	565	578	532	-160
21E	570	565	558	553	547	553	532	-64
28W	692	690	685	680	678	672	670	-44
29W	512	502	490	480	464	452	440	-128
30W	654	650	642	636	630	622	615	-68
11E	755	673	625	570	520	465	418	-528
12E	726	708	700	688	678	665	658	-120
16E	695	693	690	687	683	680	679	-30
7E	582	554	525	500	472	448	423	-254
8E	790	748	720	697	668	635	595	-272
9E	452	487	511	531	557	578	602	210
4E	578	545	522	500	480	458	442	-220
6E	898	842	803	760	710	660	600	-460
5E	270	312	342	383	421	455	481	360
1E	585	559	533	500	478	450	425	-270
2E	405	404	402	402	401	400	399	-16
3E	351	360	365	372	380	385	392	70
13E	591	592	593	593	593	593	593	4
14E	890	807	745	687	630	573	520	-574
15E	540	526	524	502	493	482	472	-116
10E	695	694	690	688	686	682	680	-28
32E	692	720	588	455	327	211	111	----
47W	1003	875	682	505	337	210	100	----

NACA

TABLE 4.- ELASTIC PROPERTIES OF SITKA SPRUCE BEAM

FROM TESTS OF COUPONS

Property[1]	Test value		Average value
	Coupon 1	Coupon 2	
Modulus of rigidity in shear (lb per sq in.)	90,560	90,820	90,690
Modulus of elasticity in compression			
E_L (lb per sq in.)	1,641,000	1,757,000	1,699,000
E_T (lb per sq in.)	34,870	40,950	37,910
Poisson's ratio			
σ_{LT}	0.46	0.50	0.48
σ_{LR}	.21	.25	.23
σ_{TL}	.01	.02	.02
σ_{TR}	.66	.66	.66

[1]L, T, and R refer to direction of grain, direction tangent to growth rings, and direction perpendicular to growth rings, respectively.

TABLE 5.– COMPUTED STRAINS IN BEAM AT 500–POUND LOAD FOR δ = 0, 0.125, AND 0.25 AND COORDINATES OF POINTS

Coordinates		Computed strain, e_{xy} (in./in.)		
x (in.)	y (in.)	δ = 0 in.	δ = 0.125 in.	δ = 0.250 in.
0.40	1.48	33.72×10^{-6}	33.25×10^{-6}	30.87×10^{-6}
.40	2.72	80.46	74.39	68.95
.40	3.25	146.22	131.15	118.17
.40	3.72	312.10	266.53	229.38
.40	4.10	777.67	610.70	488.07
.40	4.30	1490.50	1088.34	813.02
.40	4.48	2591.00	1832.24	1280.66
.40	4.52	-------	1922.92	1344.37
.40	4.56	-------	1825.47	1308.34
.40	4.60	-------	1361.33	1059.90
.40	4.66	-------	.06	.06

NACA

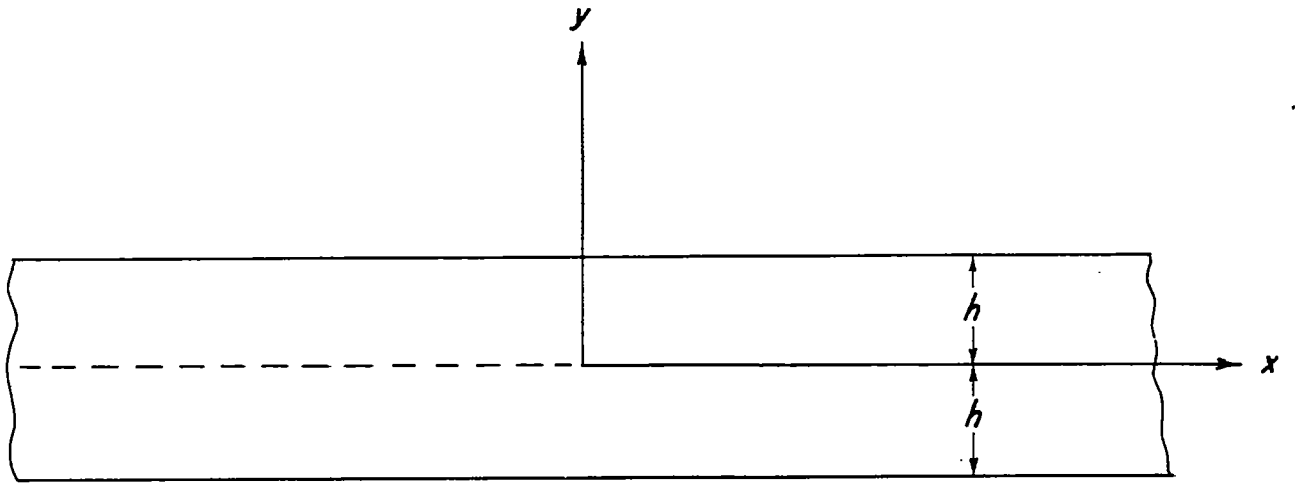

Figure 1.- Orientation of axes and dimensions of beam.

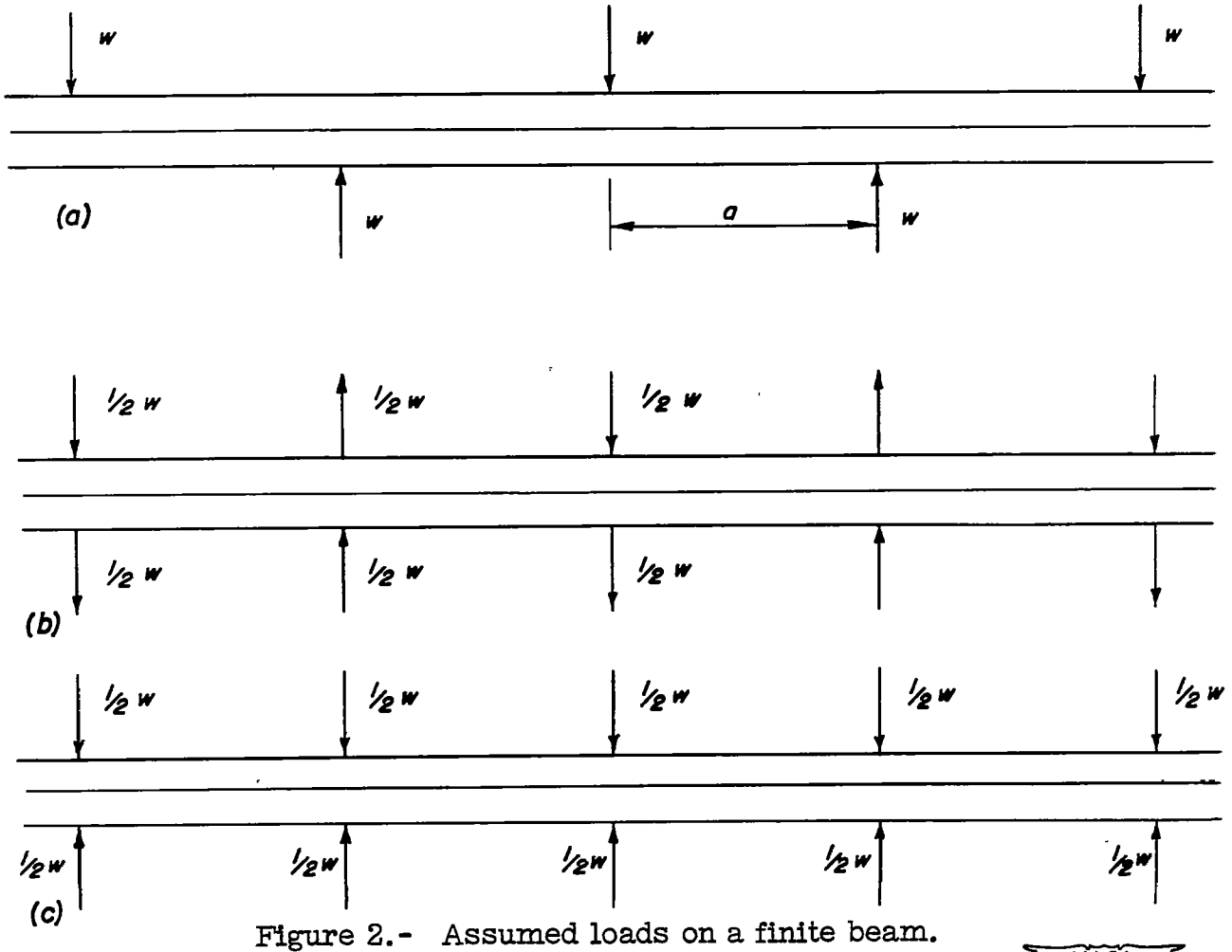

Figure 2.- Assumed loads on a finite beam.

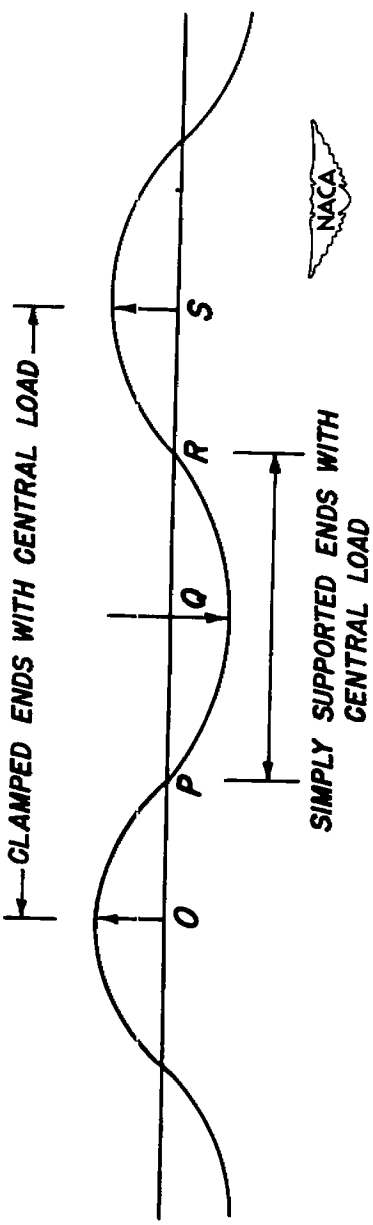

Figure 3.- Illustration of application of theory of beam of infinite length to beams of finite lengths.

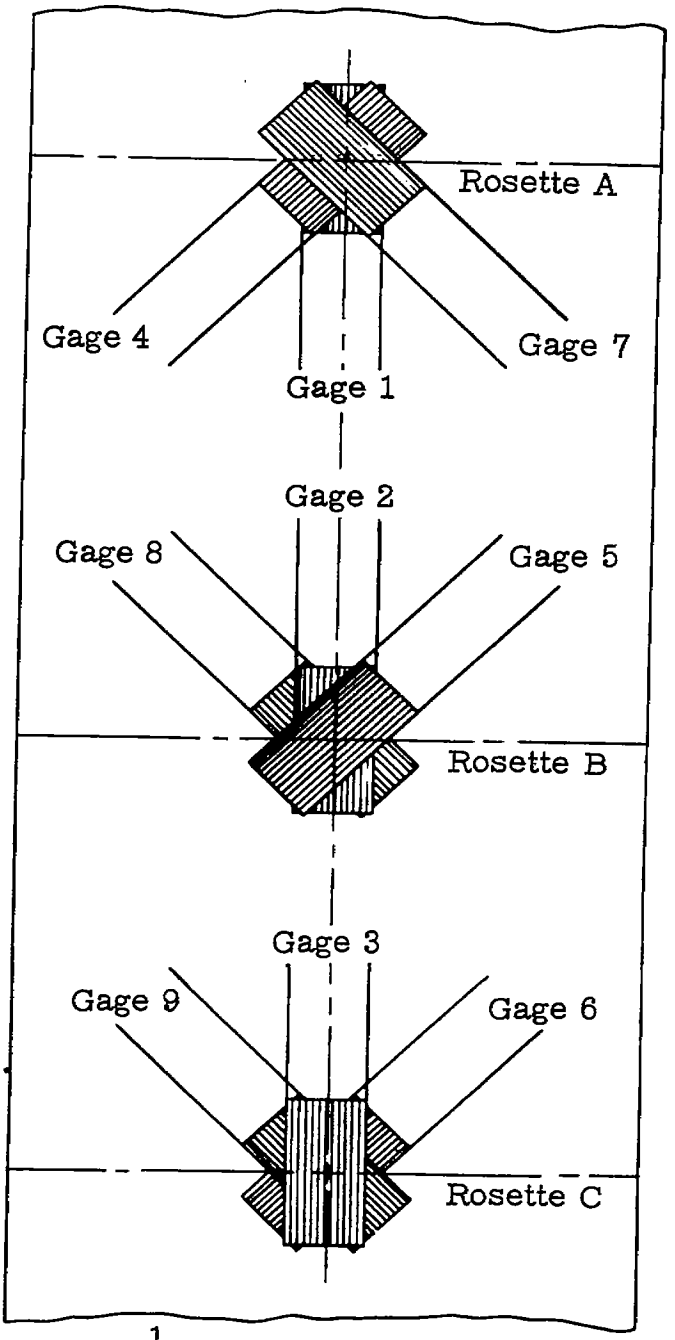

Figure 4.- Gage positions in built-up rosettes on tension specimens for check test.

NACA

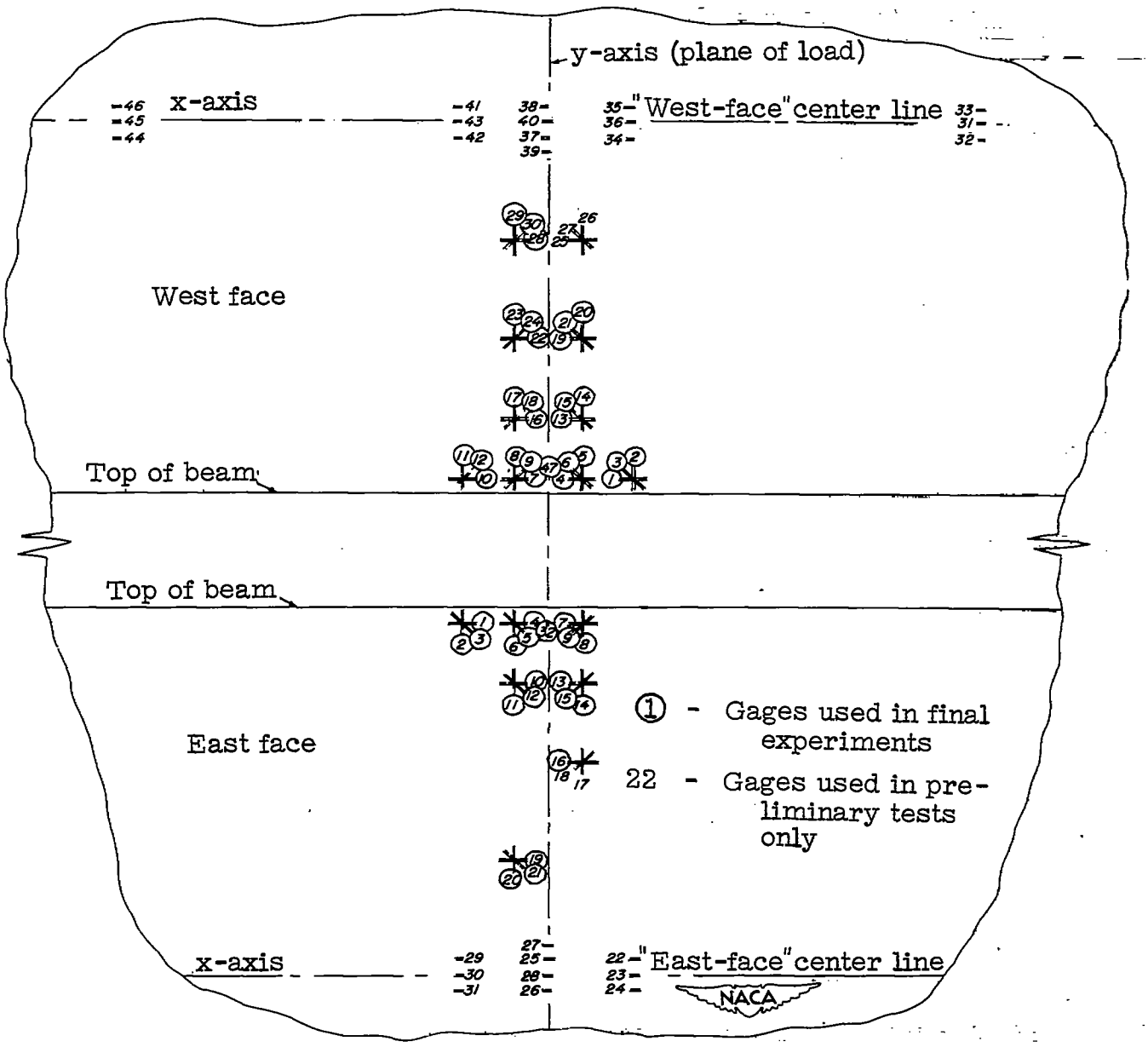

Figure 5.- Positions of electric-resistance-type strain gages on both faces of beam. (See table 2 for x- and y-coordinates of gage centers.)

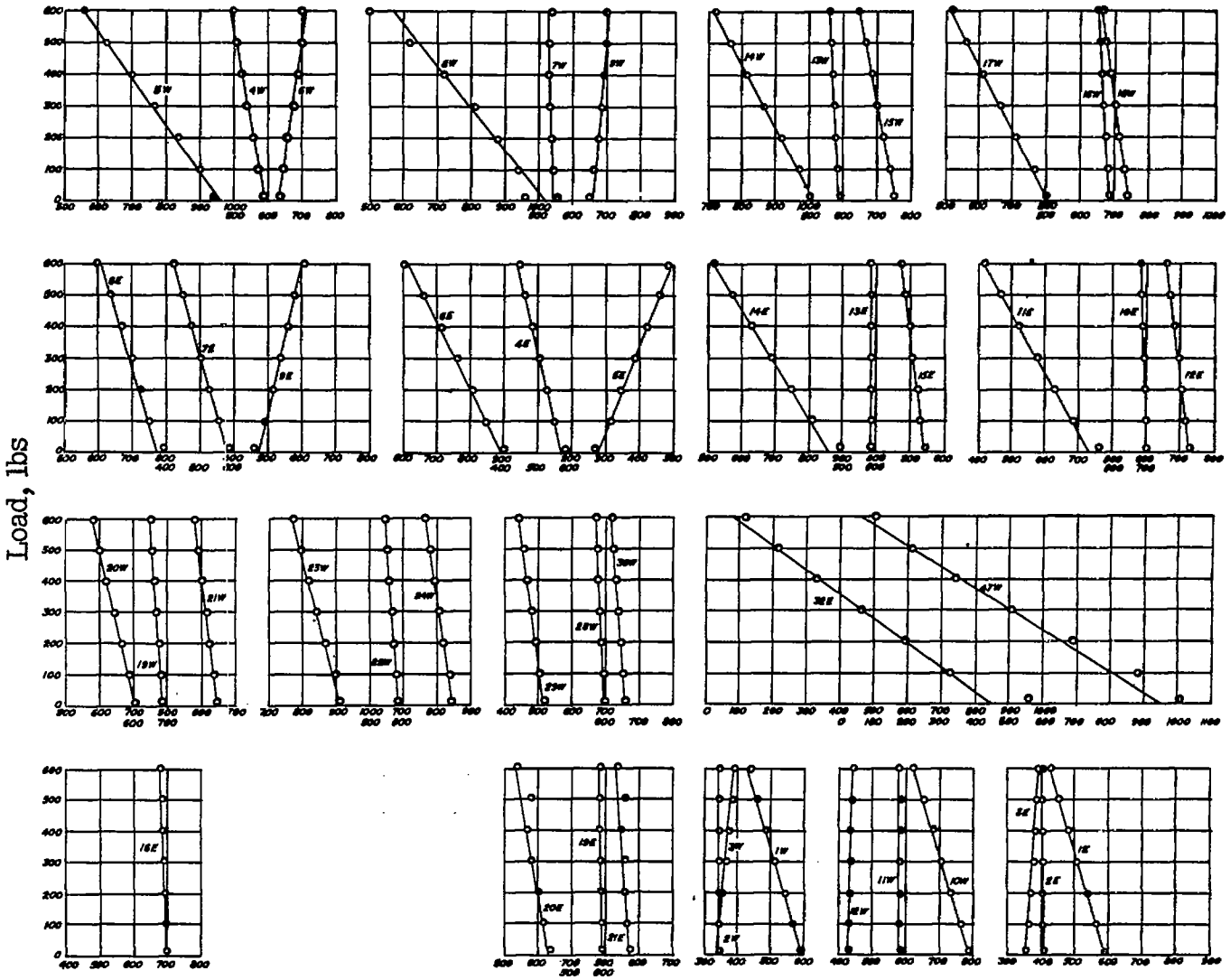

Figure 6.- Curves of load against strain for 48 gages in vicinity of load point. E, gage on east face; W, gage on west face.

NACA

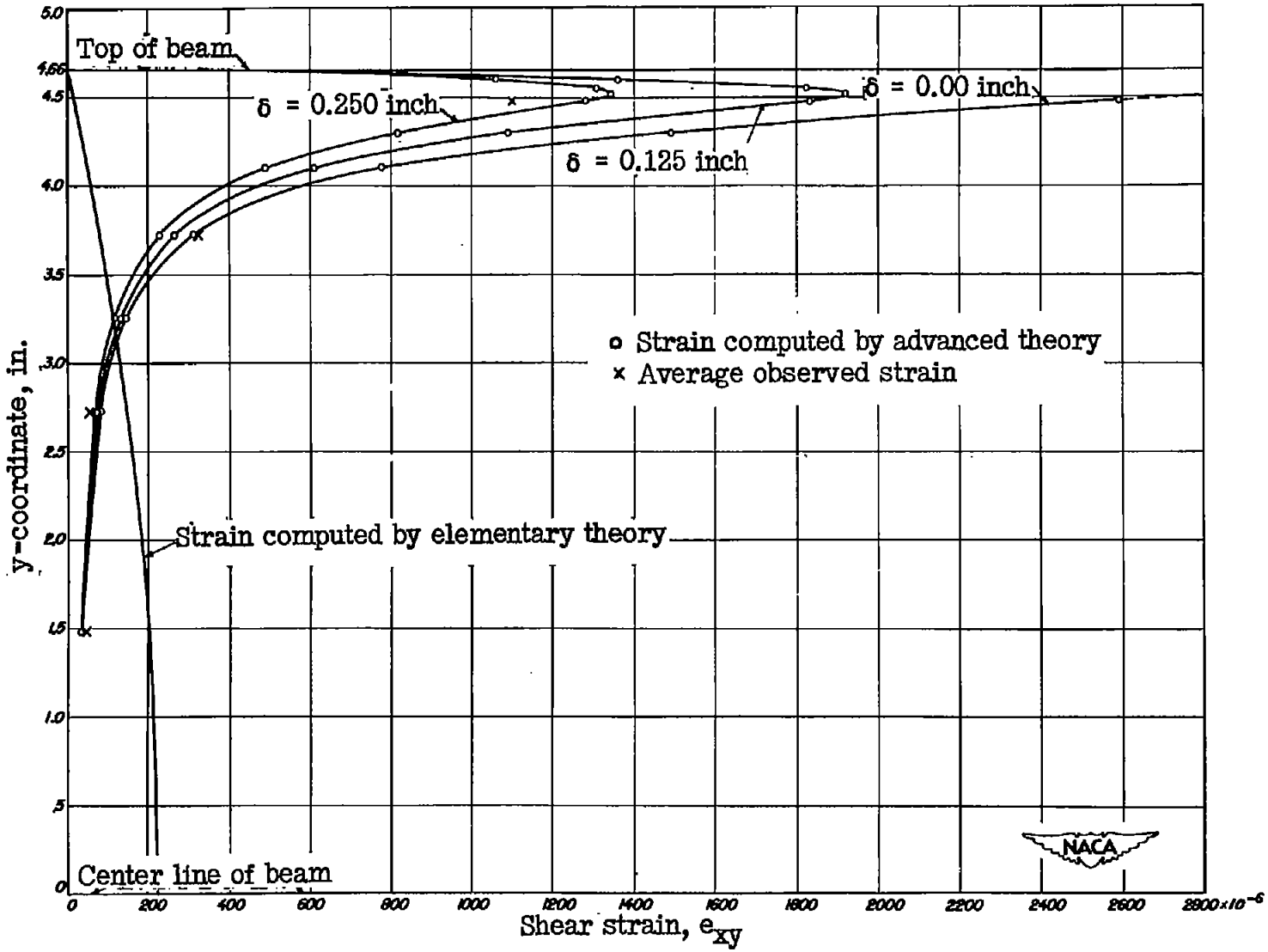

Figure 7.- Comparison of observed strains with curves showing strains computed along the line x = 0.40 from y = 0 to y = 4.66 at 500-pound center load. Both the elementary theory and the advanced mathematical theory of this report were used, with δ equal to 0.0, 0.125, and 0.250 inch.